Journal of chemical & engineering data

Article

pubs.acs.org/jced

# Densities, Viscosities, and Refractive Indexes of Good's Buffer Ionic Liquids

Sze Ying Lee,[†] Filipa A. Vicente,[‡] João A. P. Coutinho,[‡] Ianatul Khoiroh,[†] Pau Loke Show,[†] and Sónia P. M. Ventura*[,‡]

[†]Department of Chemical and Environmental Engineering, Faculty of Engineering, University of Nottingham Malaysia Campus, Jalan Broga, Semenyih 43500, Selangor Darul Ehsan, Malaysia

[‡]CICECO—Aveiro Institute of Materials, Department of Chemistry, University of Aveiro, 3810-193 Aveiro, Portugal

Supporting Information

**ABSTRACT:** Good's buffer ionic liquids (GB-ILs) have demonstrated their potential usefulness in the biotechnological field due to their advantageous properties of self-buffering and biocompatibility. To further investigate the applicability of these solvents in industrial process, the knowledge of the thermophysical properties of such solvents is of utmost importance. In this work, a series of GB-ILs prepared by the combination of the Good's buffer anions MOPSO, BES, TAPSO, and CAPSO, with tetrabutylammonium, tetrabutylphosphonium, and cholinium cations were synthesized and characterized regarding the determination of the melting and decomposition temperatures. Additionally, the physical properties such as density, viscosity and refractive index were measured for these GB-ILs at atmospheric pressure and in the (288.15 to 353.15) K temperature range. Additional properties such as the isobaric thermal expansion coefficient and activation energy for viscous flow were also further derived from the temperature dependence of the measured properties. The effects of cation and anion species of GB-ILs on these thermophysical properties are discussed.

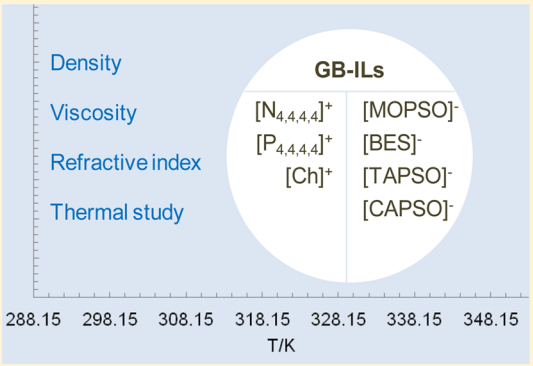


## INTRODUCTION

Ionic liquids (ILs) have emerged as a remarkable class of solvents to replace harmful volatile organic solvents due to their properties such as low volatility, nonflammability, high thermal and chemical stability, and high solvation capacity. By definition, ILs are liquids exclusively composed of ions, characterized by their low melting points below the boiling point of water. The structural variations of ions lead to a very large number of possible cation/anion combinations. By the judicious selection of these combinations, it is possible to optimize the physicochemical and thermal properties of ILs, including their density, viscosity, water and solvent miscibility, hydrophobicity, polarity, and thermal properties,[1] in order to satisfy the requirements for a specific process.[2] Therefore, over the years, new task-specific ILs are continuously being proposed.

In the biotechnological field, the biocompatibility behavior of ILs is among the primary criteria limiting their applicability in biorelated applications. High-value bioproducts such as proteins, pharmaceutical products, and amino acids are usually very labile and sensitive, being often observed the deterioration of their biological activity during the purification processes due to their contact with harmful solvents.[3] In the recent years, a new group of ILs with anions derived from Good's buffers (GBs), namely Good's buffer ionic liquids (GB-ILs),[4,5] have been synthesized and their distinctive self-buffering and biocompatibility properties imparted by their GBs anions. Additionally, GB-ILs present many beneficial characteristics such as low toxicity against the marine bacteria *Vibrio fischeri*,[4] high protein stability,[5] and capacity to form aqueous biphasic systems (ABS) with organic and inorganic salts,[4] and poly(propylene) glycol.[5] The results are promising[4,5] and ascertain the great potential of GB-ILs to be used in the biocatalysis field as stabilizing agents and simultaneously as buffering solvents.

Despite the numerous advantages reported for GB-ILs, their large-scale industrial applications will remain limited without further characterization of their thermophysical properties. Reliable thermophysical data are essential for the development and accurate design of industrial processes.[6,7] Therefore, in the present work, a series of GB-ILs in which the anions are derived from the Good's buffers MOPSO, BES, TAPSO, and CAPSO were coupled with tetrabutylammonium, tetrabutylphosphonium, and cholinium cations were synthesized by a neutralization reaction. The melting temperature and decomposition temperature of GB-ILs were determined. Additionally, the physical properties including density, viscosity, and refractive index of the GB-ILs in the temperature range

**Received:** November 6, 2015
**Accepted:** May 20, 2016
**Published:** June 3, 2016





DOI: 10.1021/acs.jced.5b00936
J. Chem. Eng. Data 2016, 61, 2260−2268

between (288.15 and 353.15) K and at atmospheric pressure were experimentally measured. The experimental data were further used for the determination of some important properties such as, the isobaric thermal expansion coefficient and the activation energy for viscous flow. The present work attempts to build the understanding on the thermophysical properties of GB-ILs composed of different combinations of cations and anions for further investigation of the potential of these solvents at an industrial level.

## EXPERIMENTAL SECTION

**Materials.** Tetrabutylammonium hydroxide solution ($w$ = 0.40 in $H_2O$), tetrabutylphosphonium hydroxide solution ($w$ = 0.40 in $H_2O$), cholinium hydroxide solution ($w$ = 0.46 in $H_2O$), 2-hydroxy-3-morpholinopropanesulfonic acid (MOPSO), 2-[bis(2-hydroxyethyl)amino]ethanesulfonic acid (BES), *N*-[tris-(hydroxymethyl)methyl]-3-amino-2-hydroxypropanesulfonic acid (TAPSO), and 3-(cyclohexylamino)-2-hydroxy-1-propanesulfonic acid (CAPSO) were supplied by Sigma-Aldrich. All the GBs used in this work have mass fractions higher than 0.99. Methanol and acetonitrile, with mass fractions higher than 0.999, were acquired from Fisher Scientific. Ultrapure water treated by a Milli-Q integral water purification system was used throughout the work.

**Synthesis and Characterization of GB-ILs.** In this work, 12 GB-ILs were synthesized by a neutralization reaction of a hydroxide solution of cations and distinct GBs. The synthesis pathway and ionic structure of cations and anions of GB-ILs are presented in Figure 1. The hydroxide solutions of tetrabutylammonium, tetrabutylphosphonium, and cholinium were added slowly to an aqueous solution slightly in excess of GBs (equimolar) and gently stirred for 12 h at room temperature. After this period, the water content in the reaction mixture was evaporated under sufficient pressure reduction and heat from an evaporator bath at 333.15 K, and using a rotary evaporator (Heidolph, model Laborota 4003 c/w rotavac vario vacuum pump), until a highly viscous liquid was obtained. The crude product was mixed with a mixture of acetonitrile and methanol in 1:1 volume ratio for tetrabutylammonium- and tetrabutylphosphonium-based GB-ILs, whereas pure methanol was used for the cholinium-based GB-ILs. Then, the solutions were stirred vigorously for 2 h at room temperature. The mixture was filtered twice to remove any free acid content. To remove the water and volatile impurities, the filtrate was dried under high vacuum with constant stirring for a minimum period of 48 h at 333.15 K or at molten state if the product was obtained as a solid salt at room temperature. The water mass fraction of the GB-ILs was determined by coulometric Karl Fischer titration (Metrohm, model 831) and was verified to be less than 0.001 by mass in all samples. The purity of all GB-ILs, shown to be higher than 0.97 in mass fraction, was checked by $^1$H and $^{13}$C nuclear magnetic resonance (NMR) spectroscopy (Bruker, model AMX 300) operating at 300 and 75 MHz (Section S1 from the Supporting Information). The specifications of the GB-ILs studied in this work are listed in Table 1.

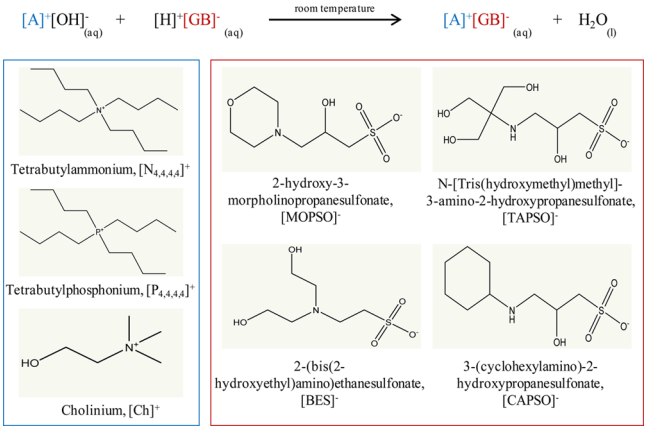


**Figure 1.** Synthesis pathway and ionic structure of cations and anions used in the GB-ILs preparation.

**Thermal Properties of GB-ILs.** The melting temperature, $T_m$, and decomposition temperature, $T_{decomp}$, of GB-ILs were determined by performing a thermal analysis on a thermogravimetric analyzer (TGA) with differential scanning calorimetric (DSC) capacity (Mettler Toledo, model TGA/DSC 1 LF) using the STAR analysis software. The samples were prepared in the aluminum pans and heated from (303.15 to 873.15) K, with a heating rate of 5 K·min$^{-1}$ and under nitrogen gas flow of 40 mL·min$^{-1}$. The standard uncertainty of temperature is 0.2 K. The melting temperatures reported from DSC data are curve peaks. Whereas, the decomposition temperatures presented are the onset temperatures, which are the intersection of the baseline below the decomposition temperature with the tangent to the mass loss versus the temperature plots in the TGA profiles. The results are expressed as the average of duplicate measurements.

**Physical Properties of GB-ILs.** *Density and Viscosity.* Measurements of density, $\rho$, and dynamic viscosity, $\eta$, in the temperature ranging from (288.15 to 353.15) K and at atmospheric pressure (≈ 0.1 MPa) were performed using an automated Stabinger viscometer (Anton Paar, model SVM 3000). The standard uncertainty of temperature and density, and the relative uncertainty of dynamic viscosity are within 0.02 K, 0.5 kg·m$^{-3}$ and 0.05, respectively. The viscometer used as well as the methodology applied for the density and viscosity measurements of the ILs studied were validated in previous works.[8,9] The viscosity standard set (Anton Paar, SH L, M, C, H) was used for the calibration of the viscometer. [$N_{4,4,4,4}$][TAPSO], [$P_{4,4,4,4}$][TAPSO], and [Ch][CAPSO] obtained are solid within the studied temperature range, and therefore, their density and viscosity could not be measured.

*Refractive Index.* The refractive index, $n_D$, was carried out at a wavelength of 589.3 nm using an automated refractometer (Anton Paar, model Abbemat 500), in the temperature range from (288.15 to 353.15) K and at atmospheric pressure. The maximum temperature deviation is 0.01 K, whereas the maximum uncertainty of the refractive index measurements is 0.0005. The equipment accuracy and the measurement methodology were previously established.[8,9] Similar to the density and viscosity measurements, nine of the 12 GB-ILs synthesized were measured, excluding [$N_{4,4,4,4}$][TAPSO], [$P_{4,4,4,4}$][TAPSO], and [Ch][CAPSO], which are solid within the measured temperature range.

## RESULTS AND DISCUSSION

**Thermal Analysis.** All the GB-ILs prepared in this work are viscous liquids at room temperature, except [$N_{4,4,4,4}$][TAPSO] ($T_m$ = 364.15 K), [$P_{4,4,4,4}$][TAPSO] ($T_m$ = 369.15 K), and [Ch][CAPSO] ($T_m$ = 365.15 K). The DSC curves used for the determination of melting temperatures of the solid GB-ILs are presented in Figure 2. The low melting temperature of the GB-ILs can be attributed to the bulky cations, [$P_{4,4,4,4}$]$^+$ and


DOI: 10.1021/acs.jced.5b00936
J. Chem. Eng. Data 2016, 61, 2260−2268

**Table 1. Specifications of the Compounds Used**

| compound | abbreviation | source | mass fraction purity | analysis method | $M$/(g·mol$^{-1}$) |
|---|---|---|---|---|---|
| tetrabutylammonium 2-hydroxy-3-morpholinopropanesulfonate | $[N_{4,4,4,4}]$[MOPSO] | synthesis | 0.99 | NMR | 466.71 |
| tetrabutylphosphonium 2-hydroxy-3-morpholinopropanesulfonate | $[P_{4,4,4,4}]$[MOPSO] | synthesis | 0.99 | NMR | 483.68 |
| cholinium 2-hydroxy-3-morpholinopropanesulfonate | [Ch][MOPSO] | synthesis | 0.97 | NMR | 328.42 |
| tetrabutylammonium 2-(bis(2-hydroxyethyl)amino)ethanesulfonate | $[N_{4,4,4,4}]$[BES] | synthesis | 0.99 | NMR | 454.70 |
| tetrabutylphosphonium 2-(bis(2-hydroxyethyl)amino)ethanesulfonate | $[P_{4,4,4,4}]$[BES] | synthesis | 0.99 | NMR | 471.67 |
| cholinium 2-(bis(2-hydroxyethyl)amino)ethanesulfonate | [Ch][BES] | synthesis | 0.97 | NMR | 316.41 |
| tetrabutylammonium *N*-[tris(hydroxymethyl)methyl]-3-amino-2-hydroxypropanesulfonate | $[N_{4,4,4,4}]$[TAPSO] | synthesis | 0.99 | NMR | 500.73 |
| tetrabutylphosphonium *N*-[tris(hydroxymethyl)methyl]-3-amino-2-hydroxypropanesulfonate | $[P_{4,4,4,4}]$[TAPSO] | synthesis | 0.99 | NMR | 517.70 |
| cholinium *N*-[tris(hydroxymethyl)methyl]-3-amino-2-hydroxypropanesulfonate | [Ch][TAPSO] | synthesis | 0.97 | NMR | 362.44 |
| tetrabutylammonium 3-(cyclohexylamino)-2-hydroxypropanesulfonate | $[N_{4,4,4,4}]$[CAPSO] | synthesis | 0.97 | NMR | 478.77 |
| tetrabutylphosphonium 3-(cyclohexylamino)-2-hydroxypropanesulfonate | $[P_{4,4,4,4}]$[CAPSO] | synthesis | 0.97 | NMR | 495.74 |
| cholinium 3-(cyclohexylamino)-2-hydroxypropanesulfonate | [Ch][CAPSO] | synthesis | 0.97 | NMR | 340.48 |

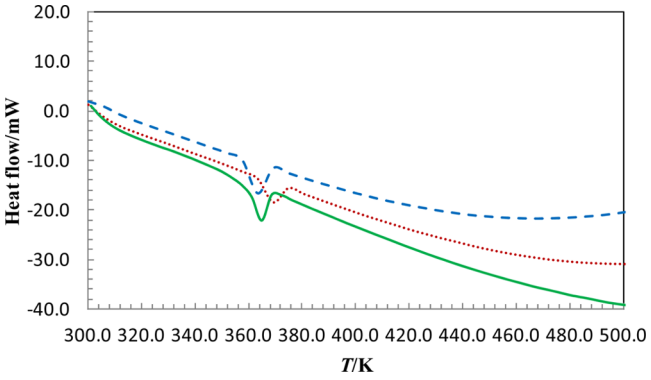


**Figure 2.** DSC curves of the solid GB-ILs: blue ---, $[N_{4,4,4,4}]$[TAPSO]; red ·····, $[P_{4,4,4,4}]$[TAPSO]; green —, [Ch][CAPSO].

$[N_{4,4,4,4}]^+$, and asymmetry of the cholinium, $[Ch]^+$, a cation with a polar hydroxyl group, paired with large anions. Unlike some GB-ILs previously reported[4] all the GB-ILs herein studied can be classified under the category of ILs by their definition, that is, salts melting below 373.15 K.

From the thermogravimetric analysis, it was observed that there is no mass loss when the solid samples melted, indicating that they have no measurable vapor pressure. The decomposition temperatures of GB-ILs are reported in Table 2, in which it is clearly seen that the initial GB-ILs decomposition temperature is identical for the different anions and appears to be dominated by the cation species. The thermal stability of the cation follows the tendency: $[Ch]^+ < [N_{4,4,4,4}]^+ < [P_{4,4,4,4}]^+$. In particular, the decomposition temperatures of tetrabutylphosphonium-based GB-ILs are between (602.15 and 612.15) K, except for $[P_{4,4,4,4}]$[TAPSO] that has a lower decomposition temperature of 548.15 K. However, this is still higher than for the tetrabutylammonium based ILs, which decompose around (541.15 to 543.15) K, whereas cholinium-based GB-ILs displayed onset decomposition temperature of (487.15 to 520.15) K. Phosphonium are generally more thermally stable than ammonium, in good agreement with literature.[10,11] Moreover, the trend of cation effect on thermal stability of ILs is in accordance with the findings of Ohno and coworkers[12,13] for amino-acid ILs (AAILs) with anions derived from L-alanine, namely tetrabutylphosphonium-based AAILs, were shown to have significantly higher thermal stability compared to tetrabutylammonium. In the same study, the authors reported that the tetraalkylammonium-based ILs with asymmetrical and shorter alkyl chains have lower thermal stability.[12,13]

**Table 2. Decomposition Temperature, $T_{decomp}$ for the GB-ILs**

| GB-ILs | $T_{decomp}$/K |
|---|---|
| $[N_{4,4,4,4}]$[MOPSO] | 541.15 |
| $[P_{4,4,4,4}]$[MOPSO] | 612.15 |
| [Ch][MOPSO] | 504.15 |
| $[N_{4,4,4,4}]$[BES] | 542.15 |
| $[P_{4,4,4,4}]$[BES] | 602.15 |
| [Ch][BES] | 500.15 |
| $[N_{4,4,4,4}]$[TAPSO] | 542.15 |
| $[P_{4,4,4,4}]$[TAPSO] | 548.15 |
| [Ch][TAPSO] | 520.15 |
| $[N_{4,4,4,4}]$[CAPSO] | 543.15 |
| $[P_{4,4,4,4}]$[CAPSO] | 611.15 |
| [Ch][CAPSO] | 487.15 |

**Density.** The experimental density data for the GB-ILs studied are depicted in Figure 3 and reported in Table 3. The density of GB-ILs decreases with the increase of the

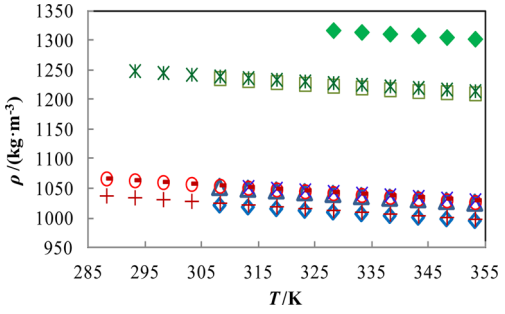


**Figure 3.** Density as a function of the temperature for GB-ILs: green ◆, [Ch]TAPSO]; green *, [Ch][BES]; green □, [Ch][MOPSO]; blue ×, $[N_{4,4,4,4}]$[BES]; red -, $[P_{4,4,4,4}]$[BES]; red ○, $[P_{4,4,4,4}]$-[MOPSO]; blue △, $[N_{4,4,4,4}]$[MOPSO]; red +, $[P_{4,4,4,4}]$[CAPSO]; blue ◇, $[N_{4,4,4,4}]$[CAPSO].



DOI: 10.1021/acs.jced.5b00936
J. Chem. Eng. Data 2016, 61, 2260−2268

Table 3. Density, $\rho$, Molar Volume, $V_m$, Viscosity, $\eta$, and Refractive Index, $n_D$, of the Studied GB-ILs as a Function of Temperature and at Pressure $p$ = 0.1 MPa[a]

| | [$N_{4,4,4,4}$][MOPSO] | | | | [$P_{4,4,4,4}$][MOPSO] | | | | [Ch][MOPSO] | | | |
|---|---|---|---|---|---|---|---|---|---|---|---|---|
| $T$/K | $\rho$/(kg·m$^{-3}$) | $10^6$ ($V_m$)/(m$^3$·mol$^{-1}$) | $\eta$/(mPa·s) | $n_D$ | $\rho$/(kg·m$^{-3}$) | $10^6$ ($V_m$)/(m$^3$·mol$^{-1}$) | $\eta$/(mPa·s) | $n_D$ | $\rho$/(kg·m$^{-3}$) | $10^6$ ($V_m$)/(m$^3$·mol$^{-1}$) | $\eta$/(mPa·s) | $n_D$ |
| 288.15 | | | | | 1066.1 | 453.7 | 22869.0 | 1.4959 | | | | |
| 293.15 | | | | | 1062.9 | 455.1 | 12430.0 | 1.4945 | | | | |
| 298.15 | | | | | 1059.9 | 456.4 | 7312.9 | 1.4930 | | | | |
| 303.15 | | | | | 1056.8 | 457.7 | 4493.6 | 1.4915 | | | | |
| 308.15 | 1051.2 | 444.0 | 34148.0 | 1.4833 | 1053.7 | 459.0 | 2859.8 | 1.4900 | 1235.3 | 265.9 | 49189.0 | 1.4978 |
| 313.15 | 1048.2 | 445.3 | 18392.0 | 1.4819 | 1050.5 | 460.4 | 1889.2 | 1.4884 | 1232.0 | 266.6 | 28090.0 | 1.4966 |
| 318.15 | 1045.3 | 446.5 | 10603.0 | 1.4804 | 1047.5 | 461.8 | 1277.0 | 1.4866 | 1228.7 | 267.3 | 16897.0 | 1.4953 |
| 323.15 | 1042.3 | 447.8 | 6381.1 | 1.4787 | 1044.4 | 463.1 | 886.7 | 1.4857 | 1225.6 | 268.0 | 10898.0 | 1.4945 |
| 328.15 | 1039.4 | 449.0 | 3976.3 | 1.4769 | 1041.3 | 464.5 | 630.4 | 1.4841 | 1222.5 | 268.7 | 6933.2 | 1.4932 |
| 333.15 | 1035.8 | 450.6 | 2571.7 | 1.4753 | 1038.2 | 465.9 | 457.8 | 1.4824 | 1219.5 | 269.3 | 4600.3 | 1.4919 |
| 338.15 | 1033.1 | 451.8 | 1702.9 | 1.4738 | 1035.1 | 467.3 | 339.2 | 1.4807 | 1216.5 | 270.0 | 3099.4 | 1.4900 |
| 343.15 | 1030.4 | 453.0 | 1158.3 | 1.4724 | 1032.1 | 468.7 | 255.6 | 1.4791 | 1213.5 | 270.7 | 2158.8 | 1.4883 |
| 348.15 | 1027.6 | 454.2 | 807.1 | 1.4711 | 1029.1 | 470.0 | 195.8 | 1.4776 | 1211.6 | 271.1 | 1545.5 | 1.4867 |
| 353.15 | 1024.7 | 455.5 | 574.9 | 1.4698 | 1026.2 | 471.4 | 152.3 | 1.4762 | 1209.7 | 271.5 | 1122.3 | 1.4852 |
| | [$N_{4,4,4,4}$][BES] | | | | [$P_{4,4,4,4}$][BES] | | | | [Ch][BES] | | | |
| $T$/K | $\rho$/(kg·m$^{-3}$) | $10^6$ ($V_m$)/(m$^3$·mol$^{-1}$) | $\eta$/(mPa·s) | $n_D$ | $\rho$/(kg·m$^{-3}$) | $10^6$ ($V_m$)/(m$^3$·mol$^{-1}$) | $\eta$/(mPa·s) | $n_D$ | $\rho$/(kg·m$^{-3}$) | $10^6$ ($V_m$)/(m$^3$·mol$^{-1}$) | $\eta$/(mPa·s) | $n_D$ |
| 288.15 | | | | 1.4909 | 1066.8 | 442.2 | 41313.0 | 1.4978 | | | | |
| 293.15 | | | | 1.4897 | 1063.9 | 443.4 | 24078.0 | 1.4964 | 1248.0 | 253.5 | 33236.0 | |
| 298.15 | | | | 1.4883 | 1061.0 | 444.6 | 14082.0 | 1.4950 | 1244.8 | 254.2 | 20518.0 | 1.5005 |
| 303.15 | | | | 1.4871 | 1058.1 | 445.8 | 8504.9 | 1.4937 | 1241.8 | 254.8 | 13056.0 | 1.4994 |
| 308.15 | | | | 1.4858 | 1055.3 | 447.0 | 5315.8 | 1.4933 | 1238.9 | 255.4 | 8631.6 | 1.4983 |
| 313.15 | 1052.4 | 432.1 | 12001.0 | 1.4845 | 1052.4 | 448.2 | 3370.9 | 1.4920 | 1236.1 | 256.0 | 5848.4 | 1.4972 |
| 318.15 | 1049.6 | 433.2 | 7582.5 | 1.4832 | 1049.6 | 449.4 | 2199.4 | 1.4906 | 1233.3 | 256.6 | 4045.8 | 1.4960 |
| 323.15 | 1046.8 | 434.4 | 4970.6 | 1.4819 | 1046.8 | 450.6 | 1356.9 | 1.4892 | 1230.5 | 257.2 | 2861.0 | 1.4948 |
| 328.15 | 1044.0 | 435.6 | 3346.6 | 1.4805 | 1044.0 | 451.8 | 871.0 | 1.4874 | 1227.7 | 257.7 | 2061.7 | 1.4932 |
| 333.15 | 1041.2 | 436.7 | 2305.7 | 1.4792 | 1041.2 | 453.0 | 611.8 | 1.4859 | 1224.9 | 258.3 | 1526.8 | 1.4915 |
| 338.15 | 1038.4 | 437.9 | 1621.8 | 1.4778 | 1038.4 | 454.2 | 458.9 | 1.4844 | 1222.2 | 258.9 | 1136.6 | 1.4905 |
| 343.15 | 1035.6 | 439.1 | 1163.2 | 1.4765 | 1035.6 | 455.5 | 352.3 | 1.4829 | 1219.5 | 259.5 | 858.1 | 1.4892 |
| 348.15 | 1032.8 | 440.3 | 848.3 | 1.4750 | 1032.8 | 456.7 | 273.6 | 1.4814 | 1216.8 | 260.1 | 658.8 | 1.4875 |
| 353.15 | 1030.1 | 441.4 | 630.0 | 1.4736 | 1030.1 | 457.9 | 214.5 | 1.4800 | 1214.1 | 260.6 | 512.7 | 1.4863 |
| | [Ch][TAPSO] | | | | [$N_{4,4,4,4}$][CAPSO] | | | | [$P_{4,4,4,4}$][CAPSO] | | | |
| $T$/K | $\rho$/(kg·m$^{-3}$) | $10^6$ ($V_m$)/(m$^3$·mol$^{-1}$) | $\eta$/(mPa·s) | $n_D$ | $\rho$/(kg·m$^{-3}$) | $10^6$ ($V_m$)/(m$^3$·mol$^{-1}$) | $\eta$/(mPa·s) | $n_D$ | $\rho$/(kg·m$^{-3}$) | $10^6$ ($V_m$)/(m$^3$·mol$^{-1}$) | $\eta$/(mPa·s) | $n_D$ |
| 288.15 | | | | | | | | | 1037.4 | 477.9 | 32956.0 | 1.4965 |
| 293.15 | | | | | | | | | 1034.2 | 479.4 | 17587.0 | 1.4950 |
| 298.15 | | | | | | | | | 1031.1 | 480.8 | 10098.0 | 1.4931 |
| 303.15 | | | | | | | | | 1028.2 | 482.2 | 6481.6 | 1.4916 |
| 308.15 | | | | | 1020.4 | 469.2 | 41227.0 | 1.4833 | 1025.1 | 483.6 | 3796.0 | 1.4898 |
| 313.15 | | | | | 1017.3 | 470.6 | 22114.0 | 1.4819 | 1022.1 | 485.0 | 2441.9 | 1.4878 |
| 318.15 | | | | | 1014.4 | 472.0 | 12579.0 | 1.4804 | 1019.0 | 486.5 | 1624.2 | 1.4872 |
| 323.15 | | | | 1.5099 | 1011.5 | 473.3 | 7480.4 | 1.4794 | 1016.0 | 488.0 | 1109.7 | 1.4855 |
| 328.15 | 1316.4 | 275.3 | 56778.0 | 1.5088 | 1008.6 | 474.7 | 4609.3 | 1.4777 | 1012.9 | 489.4 | 779.6 | 1.4837 |



J. Chem. Eng. Data 2016, 61, 2260−2268 DOI: 10.1021/acs.jced.5b00936

Table 3. continued

| | [Ch][TAPSO] | | | | [$N_{4,4,4,4}$][CAPSO] | | | | [$P_{4,4,4,4}$][CAPSO] | | | |
|---|---|---|---|---|---|---|---|---|---|---|---|---|
| $T$/K | $\rho$/(kg·m$^{-3}$) | $10^6$ ($V_m$)/(m$^3$·mol$^{-1}$) | $\eta$/(mPa·s) | $n_D$ | $\rho$/(kg·m$^{-3}$) | $10^6$ ($V_m$)/(m$^3$·mol$^{-1}$) | $\eta$/(mPa·s) | $n_D$ | $\rho$/(kg·m$^{-3}$) | $10^6$ ($V_m$)/(m$^3$·mol$^{-1}$) | $\eta$/(mPa·s) | $n_D$ |
| 333.15 | 1313.3 | 276.0 | 34168.0 | 1.5077 | 1005.7 | 476.1 | 2935.7 | 1.4762 | 1009.8 | 490.9 | 558.2 | 1.4820 |
| 338.15 | 1310.3 | 276.6 | 21501.0 | 1.5065 | 1002.8 | 477.5 | 1926.8 | 1.4745 | 1006.8 | 492.4 | 409.0 | 1.4805 |
| 343.15 | 1307.4 | 277.2 | 14013.0 | 1.5055 | 999.9 | 478.8 | 1299.4 | 1.4729 | 1003.8 | 493.9 | 304.6 | 1.4790 |
| 348.15 | 1304.6 | 277.8 | 9355.9 | 1.5044 | 997.2 | 480.1 | 898.5 | 1.4714 | 1000.9 | 495.3 | 231.0 | 1.4776 |
| 353.15 | 1301.8 | 278.4 | 6385.4 | 1.5033 | 994.3 | 481.5 | 635.7 | 1.4699 | 997.9 | 496.8 | 177.9 | 1.4763 |

[a]Standard uncertainties $u$ are $u(T)$ = 0.02 K, $u(\rho)$ = 0.5 kg·m$^{-3}$, $u_r(\eta)$ = 0.05, and $u_r(p)$ = 0.05 for density and viscosity measurements, $u(T)$ = 0.01 K, $u(n_D)$ = 0.0005 and $u_r(p)$ = 0.05 for the refractive index measurement.

temperature. Figure 4 depicts the density as a function of the molecular weight of the IL's cations at 308.15 K, with

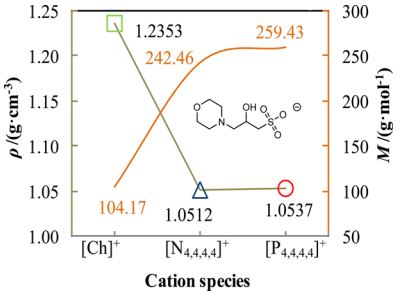


**Figure 4.** Density as a function of molecular weight of IL's cations with the common anion, [MOPSO]$^-$, at 308.15 K: green □, [Ch][MOPSO]; blue △, [$N_{4,4,4,4}$][MOPSO]; red ○, [$P_{4,4,4,4}$][MOPSO].

[MOPSO] as the common anion. From Figure 4, the results reveal that the cation imposes a pronounced effect on the density of GB-ILs, in which the density of comparable GB-ILs decreases as the bulkiness of the organic cation increases. These results are in agreement with those previously reported by us.[8,9] Cholinium-based GB-ILs with shorter alkyl side chain have higher densities than the tetrabutylammonium counterparts. Besides, it was found that the presence of phosphorus or nitrogen as cation's central atom has a small impact on the density of the studied GB-ILs. The slight cation's weight variation, due to the substitution of nitrogen by phosphorus as the cation's central atom, can be compensated by the increased molar volume of molecules due to the weaker interionic bonding.[14,15] The molar volumes of phosphonium families are generally higher than ammonium with the same anion, as depicted in Figure 5, and a small temperature dependency of

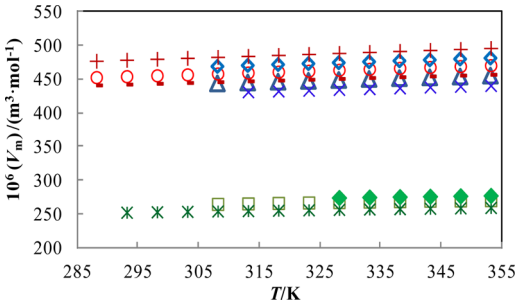


**Figure 5.** Molar volume of GB-ILs as a function of temperature: green ◆, [Ch]TAPSO]; green *, [Ch][BES]; green □, [Ch][MOPSO]; blue ×, [$N_{4,4,4,4}$][BES]; red -, [$P_{4,4,4,4}$][BES]; red ○, [$P_{4,4,4,4}$]-[MOPSO]; blue △, [$N_{4,4,4,4}$][MOPSO]; red +, [$P_{4,4,4,4}$][CAPSO]; blue ◇, [$N_{4,4,4,4}$][CAPSO].

molar volumes was observed for all the GB-ILs studied. The molar volume was calculated as described in eq 1 and reported in Table 3

$$V_m = \frac{M}{\rho} \quad (1)$$

where $V_m$ is the molar volume, $M$ is the molar mass, and $\rho$ is the density.

On the other hand, the results suggested that the density of GB-ILs, for a common cation, increases linearly with the ratio of the molecular weight and molar volume of anionic species, reflected by the predicted density of GBs: CAPSO ($\rho$ = 1300


DOI: 10.1021/acs.jced.5b00936
J. Chem. Eng. Data 2016, 61, 2260−2268

kg·m$^{-3}$) < MOPSO ($\rho$ = 1400 kg·m$^{-3}$) ≈ BES ($\rho$ = 1400 kg·m$^{-3}$) < TAPSO ($\rho$ = 1600 kg·m$^{-3}$).[16]

The experimental density data were fitted with the following empirical eq 2[17] to correlate the density as a function of temperature

$$\ln(\rho/\mathrm{kg{\cdot}m^{-3}}) = A_0 + A_1 T \quad (2)$$

where $A_0$ and $A_1$ are the fitting parameters. These fitting parameters along with the average absolute relative deviation (AARD) obtained are presented in Table 4. Despite the current

**Table 4. Correlation Parameters Obtained from Fitting of the Experimental Density Data with the Respective Average Absolute Relative Deviation at Pressure $p$ = 0.1 MPa[a]**

| GB-ILs | $A_0 \pm \sigma$ | $10^4$ ($A_1 \pm \sigma$)/K$^{-1}$ | AARD[b]/% |
|---|---|---|---|
| [$N_{4,4,4,4}$][MOPSO] | 7.1334 ± 0.0015 | −5.7040 ± 0.0047 | 0.0156 |
| [$P_{4,4,4,4}$][MOPSO] | 7.1414 ± 0.0003 | −5.8868 ± 0.0007 | 0.0047 |
| [Ch][MOPSO] | 7.2651 ± 0.0040 | −4.7565 ± 0.0121 | 0.0420 |
| [$N_{4,4,4,4}$][BES] | 7.1269 ± 0.0002 | −5.3656 ± 0.0006 | 0.0029 |
| [$P_{4,4,4,4}$][BES] | 7.1275 ± 0.0002 | −5.3848 ± 0.0005 | 0.0030 |
| [Ch][BES] | 7.2626 ± 0.0007 | −4.5598 ± 0.0022 | 0.0107 |
| [Ch][TAPSO] | 7.3287 ± 0.0015 | −4.4525 ± 0.0043 | 0.0076 |
| [$N_{4,4,4,4}$][CAPSO] | 7.1047 ± 0.0005 | −5.7415 ± 0.0016 | 0.0053 |
| [$P_{4,4,4,4}$][CAPSO] | 7.1165 ± 0.0003 | −5.9722 ± 0.0009 | 0.0067 |
| overall AARD[c]/% | | | 0.0109 |

[a]Standard uncertainties $u$ are $u(T)$ = 0.02 K, $u(\rho)$ = 0.5 kg·m$^{-3}$ and $u_r(p)$ = 0.05. [b]AARD = $\frac{100}{n}\sum_{k=1}^{n}\frac{|\rho_k^{exp}-\rho_k^{cal}|}{\rho_k^{exp}}$, where $n$ is the number of data points, and the superscript "exp" and "cal" are the experimental and calculated values, respectively. [c]Overall AARD = $\frac{100}{N}\sum_{k=1}^{N}\frac{|\rho_k^{exp}-\rho_k^{cal}|}{\rho_k^{exp}}$, where $N$ is the total number of data points.

debate regarding the application of a linear correlation or a second order polynomial equation to describe the temperature dependency of density of ILs, for which this work cannot provide an answer, the experimental data are well described by eq 2, with a very small value of overall AARD of 0.0109%.

The temperature dependency of the density was further used to determine the isobaric thermal expansion coefficient, $\alpha$, according to eq 3[17]

$$\alpha = -\frac{1}{\rho}\left(\frac{\partial\rho}{\partial T}\right)_p = -\left(\frac{\partial \ln\rho}{\partial T}\right)_p = -A_1 \quad (3)$$

In the temperature range of (288.15 to 353.15) K, the thermal expansion coefficients of the studied GB-ILs are in a narrow range, in more particular, (4.45 to 4.76) × 10$^{-4}$ K$^{-1}$ for cholinium family, (5.37 to 5.74) × 10$^{-4}$ K$^{-1}$ for ammonium family, and (5.38 to 5.97) × 10$^{-4}$ K$^{-1}$ for phosphonium family. The thermal expansion coefficient increases in the following GB-ILs cation sequence: $[Ch]^+$ < $[N_{4,4,4,4}]^+$ < $[P_{4,4,4,4}]^+$. This can be attributed to the ILs with large cation size having weaker electrostatic interactions and thus facilitating their thermal expansion.[18] Despite the effect of cation on the thermal expansion coefficients, the anion moieties of GB-ILs affect the thermal expansion coefficient in the following rank: $[TAPSO]^-$ < $[BES]^-$ < $[MOPSO]^-$ < $[CAPSO]^-$. The $\alpha$ values obtained for the GB-ILs are in good agreement with those reported for the same ILs families.[8,9,19]

**Viscosity.** The viscosity for GB-ILs was measured from (288.15 to 353.15) K at atmospheric pressure and the results are presented in Figure 6 (see Table 3 for detailed values). In contrast to density, a temperature increase has a dramatic

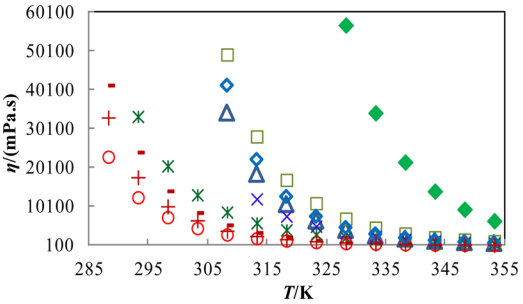


**Figure 6.** Viscosity of GB-ILs as a function of temperature: green ◆, [Ch]TAPSO]; green *, [Ch][BES]; green □, [Ch][MOPSO]; blue ×, [$N_{4,4,4,4}$][BES]; red -, [$P_{4,4,4,4}$][BES]; red ○, [$P_{4,4,4,4}$][MOPSO]; blue △, [$N_{4,4,4,4}$][MOPSO]; red +, [$P_{4,4,4,4}$][CAPSO]; green ◇, [$N_{4,4,4,4}$]-[CAPSO].

impact on the dynamic viscosity. The GB-ILs viscosity decreases drastically when increasing the temperature. It is well established that the chemical structure of the ILs anions has a strong influence on the viscosity.[20] Particularly, the ILs viscosity is essentially governed by the strength of their van der Waals interactions and their capacity to form hydrogen bonds.[1] All the GB-ILs studied exhibit remarkably high viscosities at room temperature, compared to traditional room temperature ILs. This can be attributed to the large size of anions and the presence of several H-bond acceptors and donors in the anion structures, resulting in the increase of the liquid intermolecular forces and, thus, making GB-ILs more viscous. Table 5 presents

**Table 5. H-Bond Formation Tendency of Anion Species of GB-ILs**

| anions | no. of H-bond acceptor | no. of H-bond donor |
|---|---|---|
| $[MOPSO]^-$ | 6 | 1 |
| $[BES]^-$ | 6 | 2 |
| $[TAPSO]^-$ | 8 | 5 |
| $[CAPSO]^-$ | 5 | 2 |

the number of H-bond acceptors and donors within the several anions of the GB-ILs, which impacts significantly on the varied viscosity of GB-ILs observed. Moreover, despite the effect of the anionic structure, cholinium containing a hydroxyl group at the alkyl side chain yields a higher viscosity, except for [Ch][BES]. The extremely high viscosity of [Ch][TAPSO] may be attributed to the additional hydrogen bonding interactions involving the functional groups of the cations[21] with other cations or $[TAPSO]^-$ anions having high hydrogen-bonding formation capacity. On the other hand, the phosphonium family has relatively lower viscosities than those of the corresponding ammonium GB-ILs with the same anions. This behavior has been validated by several researchers[14,15] using different approaches. These works explained that the substitution of a heavy atom within the cation core provides a weaker interionic interaction,[14] which in turn results in a reduced viscosity.

The high viscosity of ILs might negatively affect the mass transfer rate and process operating conditions. However, the viscosity can be lowered markedly by increasing the temperature or by the addition of small amounts of organic solvents[22]


DOI: 10.1021/acs.jced.5b00936
J. Chem. Eng. Data 2016, 61, 2260−2268

Table 6. Correlation Parameters Obtained from Fitting of the Experimental Viscosity Data Using the VTF Equation and the Respective Average Absolute Relative Deviation at Pressure of 0.1 MPa[a]

| GB-ILs | $A_\eta \pm \sigma$ | $B_\eta \pm \sigma$/K | $T_{0\eta} \pm \sigma$/K | AARD[b]/% |
|---|---|---|---|---|
| $[N_{4,4,4,4}][MOPSO]$ | −4.1270 ± 0.1866 | 1686.6 ± 50.8 | 192.3 ± 2.0 | 0.3856 |
| $[P_{4,4,4,4}][MOPSO]$ | −3.5281 ± 0.1098 | 1509.8 ± 30.7 | 176.7 ± 1.4 | 0.5026 |
| [Ch][MOPSO] | −3.9791 ± 0.4206 | 1937.4 ± 127.6 | 177.0 ± 5.0 | 0.7094 |
| $[N_{4,4,4,4}][BES]$ | −4.3409 ± 0.1441 | 2013.3 ± 47.6 | 166.5 ± 1.9 | 0.1596 |
| $[P_{4,4,4,4}][BES]$ | −5.4171 ± 0.8407 | 2073.4 ± 195.4 | 159.4 ± 7.3 | 0.9985 |
| [Ch][BES] | −3.5247 ± 0.0963 | 1960.7 ± 32.3 | 152.4 ± 1.4 | 0.2383 |
| [Ch][TAPSO] | −2.3696 ± 0.1885 | 1699.7 ± 136.2 | 200.5 ± 5.6 | 0.2608 |
| $[N_{4,4,4,4}][CAPSO]$ | −4.4239 ± 0.0952 | 1767.9 ± 26.2 | 190.7 ± 1.0 | 0.1883 |
| $[P_{4,4,4,4}][CAPSO]$ | −3.9009 ± 0.2797 | 1616.5 ± 79.1 | 175.1 ± 3.4 | 0.9187 |
| overall AARD[c]/% | | | | 0.4846 |

[a]Standard uncertainties $u$ are $u(T) = 0.02$ K, $u_r(\eta) = 0.05$, and $u_r(p) = 0.05$. [b]$\text{AARD} = \frac{100}{n}\sum_{k=1}^{n}\frac{|\eta_k^{exp} - \eta_k^{cal}|}{\eta_k^{exp}}$, where $n$ is the number of data points, and the superscript "exp" and "cal" are the experimental and calculated values, respectively. [c]$\text{Overall AARD} = \frac{100}{N}\sum_{k=1}^{N}\frac{|\eta_k^{exp} - \eta_k^{cal}|}{\eta_k^{exp}}$, where $N$ is the total number of data points.

or water.[23] Besides, water miscible GB-ILs are used in the form of water−GB-ILs mixture in most applications of biotechnological field.

The temperature dependence of dynamic viscosity of GB-ILs was correlated using the Vogel−Tammann−Fulcher (VTF) model described in eq 4

$$\ln(\eta/\text{mPa·s}) = A_\eta + \frac{B_\eta}{T - T_{0\eta}} \quad (4)$$

where $A_\eta$, $B_\eta$, and $T_{0\eta}$ are the adjustable parameters estimated by the fitting from the experimental data. The experimental dynamic viscosity data are well fitted to the VTF model. The best fitting parameters are presented in Table 6 along with the overall AARD of 0.4846%.

The experimental viscosity data were also fitted to the Arrhenius equation as expressed in eq 5[24]

$$\ln(\eta/\text{mPa·s}) = \ln(\eta_\infty/\text{mPa·s}) + \frac{E_\eta}{RT} \quad (5)$$

where $\eta_\infty$ is the dynamic viscosity at infinite temperature, $E_\eta$ is the activation energy for viscous flow in J·mol$^{-1}$, and $R$ is the gas universal constant. The values of $E_\eta$ and $\eta_\infty$ are reported in Table 7. Although the experimental data are fitted with the Arrhenius equation satisfactorily with small AARD values of 0.7709%, the Arrhenius plot was not linear, in particular for tetrabutylphosphonium-based GB-ILs, those represented by the highest molar mass.[25] This nonlinear temperature dependence of viscosity has been reported for several ILs.[17,24,25] By comparing the values of AARD for the VTF and Arrhenius equations, respectively, the temperature dependence for viscosity of GB-ILs is better to be described by the VTF model.

Despite the fact that the Arrhenius plot is not exactly linear, by considering the satisfactory level of AARD values obtained, the values of the activation energy and dynamic viscosity at infinite temperature were calculated from the slope and intercept of the Arrhenius plot, as a first approximation to compare with the literature data. The activation energy can be described as the energy barrier which must be overcome for the ions to move past each other in the ionic fluid.[25] Compared to the ILs reported,[17,24,25] the activation energy values of GB-ILs are significantly higher due to the presence of strong interactions of ions occurring in the ionic fluid, caused by the high hydrogen formation strength associated with the anions or cations. On the other hand, the dynamic viscosity at infinite temperature can be used to describe purely the structural contribution of the ions to the viscosity, since the related ions interactions contributing to the viscosity at room temperature will not be effective at infinite temperature. From Table 7, it was observed the decrease of $\eta_\infty$ with the increase of $E_\eta$, being this finding in accordance with previous studies conducted by Okoturo and VanderNoot,[25] which suggests that the van der Waals interactions, molar mass, and symmetry effects that commonly contribute to the viscosity at the room temperature may not be significant at infinite temperature.

Table 7. Activation Energy and Infinite Temperature Viscosity Obtained from Fitting of the Experimental Viscosity Data Using the Arrhenius Equation and the Respective Average Absolute Relative Deviation at Pressure of 0.1 MPa[a]

| GB-ILs | $E_\eta$/(kJ·mol$^{-1}$) | $10^6$ $(\eta_\infty)$/(mPa·s) | AARD[b]/% |
|---|---|---|---|
| $[N_{4,4,4,4}][MOPSO]$ | 81.55 | 0.0004 | 0.7383 |
| $[P_{4,4,4,4}][MOPSO]$ | 64.39 | 0.0385 | 1.0187 |
| [Ch][MOPSO] | 75.67 | 0.0066 | 0.5458 |
| $[N_{4,4,4,4}][BES]$ | 67.53 | 0.0616 | 0.3625 |
| $[P_{4,4,4,4}][BES]$ | 69.87 | 0.0079 | 1.3748 |
| [Ch][BES] | 59.47 | 0.7463 | 0.6463 |
| [Ch][TAPSO] | 83.98 | 0.0024 | 0.2060 |
| $[N_{4,4,4,4}][CAPSO]$ | 83.45 | 0.0003 | 0.7378 |
| $[P_{4,4,4,4}][CAPSO]$ | 67.34 | 0.0163 | 1.3076 |
| overall AARD[c]/% | | | 0.7709 |

[a]Standard uncertainties $u$ are $u(T) = 0.02$ K, $u_r(\eta) = 0.05$, and $u_r(p) = 0.05$. [b]$\text{AARD} = \frac{100}{n}\sum_{k=1}^{n}\frac{|\eta_k^{exp} - \eta_k^{cal}|}{\eta_k^{exp}}$, where $n$ is the number of data points, and the superscript "exp" and "cal" are the experimental and calculated values, respectively. [c]$\text{Overall AARD} = \frac{100}{N}\sum_{k=1}^{N}\frac{|\eta_k^{exp} - \eta_k^{cal}|}{\eta_k^{exp}}$, where $N$ is the total number of data points.

**Refractive Index.** The refractive indices as a function of temperature for GB-IL are presented in Table 3 and depicted in Figure 7. A linear decrease with the temperature was observed and the experiment results were correlated with the following empirical eq 6[19,26]

$$n_D = B_0 + B_1 T \quad (6)$$



DOI: 10.1021/acs.jced.5b00936
J. Chem. Eng. Data 2016, 61, 2260−2268

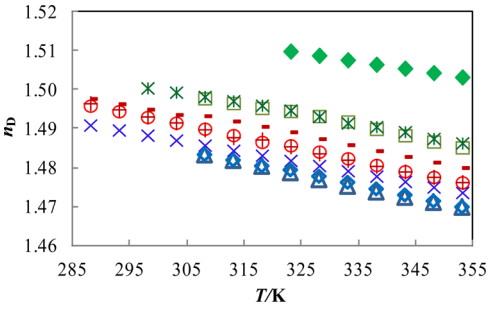


**Figure 7.** Refractive index of GB-ILs as a function of temperature: green ◆, [Ch]TAPSO]; green *, [Ch][BES]; green □, [Ch]-[MOPSO]; blue ×, [$N_{4,4,4,4}$][BES]; red -, [$P_{4,4,4,4}$][BES]; red ○, [$P_{4,4,4,4}$][MOPSO]; blue △, [$N_{4,4,4,4}$][MOPSO]; red +, [$P_{4,4,4,4}$]-[CAPSO]; blue ◇, [$N_{4,4,4,4}$][CAPSO].

where $B_0$ and $B_1$ are the fitting parameters. The optimal fitting parameters along with the AARD obtained are reported in Table 8. In general, a good agreement was observed between

**Table 8. Correlation Parameters Obtained from Fitting of the Experimental Refractive Index Data and the Respective Average Absolute Relative Deviation at Pressure of 0.1 MPa[a]**

| GB-ILs | $B_0 \pm \sigma$ | $10^4$ ($B_1 \pm \sigma$)/$K^{-1}$ | AARD[b]/% |
|---|---|---|---|
| [$N_{4,4,4,4}$][MOPSO] | 1.5777 ± 0.0018 | −3.0635 ± 0.0536 | 0.0123 |
| [$P_{4,4,4,4}$][MOPSO] | 1.5839 ± 0.0008 | −3.0509 ± 0.0236 | 0.0085 |
| [Ch][MOPSO] | 1.5851 ± 0.0033 | −2.8167 ± 0.0983 | 0.0242 |
| [$N_{4,4,4,4}$][BES] | 1.5675 ± 0.0004 | −2.6519 ± 0.0121 | 0.0050 |
| [$P_{4,4,4,4}$][BES] | 1.5770 ± 0.0020 | −2.7340 ± 0.0620 | 0.0269 |
| [Ch][BES] | 1.5789 ± 0.0015 | −2.6172 ± 0.0469 | 0.0150 |
| [Ch][TAPSO] | 1.5814 ± 0.0004 | −2.2132 ± 0.0132 | 0.0028 |
| [$N_{4,4,4,4}$][CAPSO] | 1.5762 ± 0.0015 | −3.0073 ± 0.0451 | 0.0111 |
| [$P_{4,4,4,4}$][CAPSO] | 1.5865 ± 0.0012 | −3.1305 ± 0.0370 | 0.0137 |
| overall AARD[c]/% | | | 0.0133 |

[a]Standard uncertainties $u$ are $u(T)$ = 0.01 K, $u(n_D)$ = 0.0005, $u_r(p)$ = 0.05. [b]$\mathrm{AARD} = \frac{100}{n}\sum_{k=1}^{n}\frac{|n_{D_k}^{exp} - n_{D_k}^{cal}|}{n_{D_k}^{exp}}$, where $n$ is the number of data points, and the superscript "exp" and "cal" are the experimental and calculated values, respectively. [c]$\mathrm{Overall\ AARD} = \frac{100}{N}\sum_{k=1}^{N}\frac{|n_{D_k}^{exp} - n_{D_k}^{cal}|}{n_{D_k}^{exp}}$, where $N$ is the total number of data points.

the experimental data and fitting data with overall AARD values of 0.0133%. The refractive index of GB-ILs covers a very narrow window (1.47 to 1.52) in the temperature range of (288.15 to 353.15) K. It was found that the refractive index of an IL depends on the nature of both the cation and anion, as we have previously reported.[8,9] In this study, the refractive indices of GB-ILs increase in the following cationic sequence: $[N_{4,4,4,4}]^+ < [P_{4,4,4,4}]^+ < [Ch]^+$, and for the same cation, follow the anionic order: $[MOPSO]^- < [CAPSO]^- < [BES]^- < [TAPSO]^-$.

## CONCLUSIONS

In this work, a series of GB-ILs incorporating different combinations of cations and GBs anions were synthesized and their thermophysical properties were investigated in detail at atmospheric pressure. The GB-ILs synthesized exhibit good thermal stability, indicating the wide useful liquid range for their applications. Additionally, the physical properties including density, viscosity, and refractive index as a function of temperature were measured and correlated with the empirical equations to describe the temperature dependence of these physical properties. The GB-ILs viscosity decreases drastically when increasing the temperature, whereas their density demonstrated a linear dependency between $\ln \rho$ and temperature. The results evidence that the cation imposes a pronounced effect on the density of GB-ILs; thus, the density of comparable GB-ILs decreases as the bulkiness of the organic cation increases. Meanwhile, the low melting temperature of the GB-ILs were in this particular case attributed to the bulky cations, $[P_{4,4,4,4}]^+$ and $[N_{4,4,4,4}]^+$, and asymmetry of the cholinium cation. Furthermore, the experimental data were used for the derivation of some additional thermodynamics parameters, such as the isobaric thermal expansion coefficient and activation energy for viscous flow.

The study of the thermophysical properties and the cation/anion structure−property relationship of GB-ILs can be beneficial in the design of new GB-ILs and further investigation of their applications.

## ASSOCIATED CONTENT

### Supporting Information

The Supporting Information is available free of charge on the ACS Publications website at DOI: 10.1021/acs.jced.5b00936.

NMR analysis of GB-ILs. (PDF)

## AUTHOR INFORMATION

### Corresponding Author

*E-mail: spventura@ua.pt. Fax: +351 234 370 084. Tel.: +351 234 401 507.

### Funding

This research was supported by Malaysia Toray Science Foundation ref TML-CA/15.169 and Fundamental Research Grant Scheme ref FRGS/1/2015/SG05/UNIM/03/1. L.S.Y. gratefully acknowledges MyBrain 15 Scholarship from the Ministry of Higher Education (MOHE), Malaysia. The authors also acknowledge FEDER funds through the program COMPETE and for national fund through the Portuguese Foundation for Science and Technology (FCT) for CICECO-Aveiro Institute of Materials ref. FCT UID/CTM/50011/2013 and the research project PTDC/ATP-EAM/5331/2014. We thank the FCT for doctoral grants SFRH/BD/101683/2014 (to F.A.V.) and for the postdoctoral grant SFRH/BPD/79263/2011 (to S.P.M.V).

### Notes

The authors declare no competing financial interest.

## REFERENCES

(1) Zhang, S.; Sun, N.; He, X.; Lu, X.; Zhang, X. Physical properties of ionic liquids: database and evaluation. *J. Phys. Chem. Ref. Data* **2006**, *35*, 1475−1517.

(2) Plechkova, N. V.; Seddon, K. R. Applications of ionic liquids in the chemical industry. *Chem. Soc. Rev.* **2008**, *37*, 123−150.

(3) Carta, G.; Jungbauer, A. *Protein chromatography: process development and scale-up*; John Wiley & Sons: Weinheim Germany, 2010.

(4) Taha, M.; e Silva, F. A.; Quental, M. V.; Ventura, S. P.; Freire, M. G.; Coutinho, J. A. Good's buffers as a basis for developing self-buffering and biocompatible ionic liquids for biological research. *Green Chem.* **2014**, *16*, 3149−3159.

(5) Taha, M.; Quental, M. V.; Correia, I.; Freire, M. G.; Coutinho, J. A. P. Extraction and stability of bovine serum albumin (BSA) using



DOI: 10.1021/acs.jced.5b00936
J. Chem. Eng. Data 2016, 61, 2260−2268

cholinium-based Good's buffers ionic liquids. *Process Biochem.* **2015**, *50*, 1158−1166.
(6) França, J. M. P.; Nieto de Castro, C. A.; Lopes, M. M.; Nunes, V. M. B. Influence of Thermophysical Properties of Ionic Liquids in Chemical Process Design. *J. Chem. Eng. Data* **2009**, *54*, 2569−2575.
(7) Aparicio, S.; Atilhan, M.; Karadas, F. Thermophysical Properties of Pure Ionic Liquids: Review of Present Situation. *Ind. Eng. Chem. Res.* **2010**, *49*, 9580−9595.
(8) Bhattacharjee, A.; Lopes-da-Silva, J. A.; Freire, M. G.; Coutinho, J. A. P.; Carvalho, P. J. Thermophysical properties of phosphonium-based ionic liquids. *Fluid Phase Equilib.* **2015**, *400*, 103−113.
(9) Bhattacharjee, A.; Luis, A.; Lopes-da-Silva, J. A.; Freire, M. G.; Carvalho, P. J.; Coutinho, J. A.; Santos, J. H. Thermophysical properties of sulfonium- and ammonium-based ionic liquids. *Fluid Phase Equilib.* **2014**, *381*, 36−45.
(10) Luo, J.; Conrad, O.; Vankelecom, I. F. J. Physicochemical properties of phosphonium-based and ammonium-based protic ionic liquids. *J. Mater. Chem.* **2012**, *22*, 20574−20579.
(11) Bradaric, C. J.; Downard, A.; Kennedy, C.; Robertson, A. J.; Zhou, Y. Industrial preparation of phosphonium ionic liquids. *Green Chem.* **2003**, *5*, 143−152.
(12) Ohno, H.; Fukumoto, K. Amino acid ionic liquids. *Acc. Chem. Res.* **2007**, *40*, 1122−1129.
(13) Kagimoto, J.; Fukumoto, K.; Ohno, H. Effect of tetrabutylphosphonium cation on the physico-chemical properties of amino-acid ionic liquids. *Chem. Commun.* **2006**, 2254−2256.
(14) Shirota, H.; Fukazawa, H.; Fujisawa, T.; Wishart, J. F. Heavy Atom Substitution Effects in Non-Aromatic Ionic Liquids: Ultrafast Dynamics and Physical Properties. *J. Phys. Chem. B* **2010**, *114*, 9400−9412.
(15) Tsunashima, K.; Sugiya, M. Physical and electrochemical properties of low-viscosity phosphonium ionic liquids as potential electrolytes. *Electrochem. Commun.* **2007**, *9*, 2353−2358.
(16) ChemSpider. http://www.chemsipider.com/ (accessed June 10, 2015).
(17) Liu, Q.-S.; Liu, J.; Liu, X.-X.; Zhang, S.-T. Density, dynamic viscosity, and electrical conductivity of two hydrophobic functionalized ionic liquids. *J. Chem. Thermodyn.* **2015**, *90*, 39−45.
(18) Neves, C. M.; Kurnia, K. A.; Coutinho, J. A.; Marrucho, I. M.; Lopes, J. N.; Freire, M. G.; Rebelo, L. P. Systematic study of the thermophysical properties of imidazolium-based ionic liquids with cyano-functionalized anions. *J. Phys. Chem. B* **2013**, *117*, 10271−10283.
(19) Tao, D.-J.; Cheng, Z.; Chen, F.-F.; Li, Z.-M.; Hu, N.; Chen, X.-S. Synthesis and Thermophysical Properties of Biocompatible Cholinium-Based Amino Acid Ionic Liquids. *J. Chem. Eng. Data* **2013**, *58*, 1542−1548.
(20) Fraser, K. J.; MacFarlane, D. R. Phosphonium-based ionic liquids: An overview. *Aust. J. Chem.* **2009**, *62*, 309−321.
(21) Zhang, Y.; Li, T.; Wu, Z.; Yu, P.; Luo, Y. Synthesis and thermophysical properties of imidazolate-based ionic liquids: Influences of different cations and anions. *J. Chem. Thermodyn.* **2014**, *74*, 209−215.
(22) Liao, Q.; Hussey, C. L. Densities, Viscosities, and Conductivities of Mixtures of Benzene with the Lewis Acidic Aluminum Chloride + 1-Methyl-3-ethylimidazolium Chloride Molten Salt. *J. Chem. Eng. Data* **1996**, *41*, 1126−1130.
(23) Kelkar, M. S.; Maginn, E. J. Effect of temperature and water content on the shear viscosity of the ionic liquid 1-ethyl-3-methylimidazolium bis (trifluoromethanesulfonyl) imide as studied by atomistic simulations. *J. Phys. Chem. B* **2007**, *111*, 4867−4876.
(24) Panda, S.; Gardas, R. L. Measurement and correlation for the thermophysical properties of novel pyrrolidonium ionic liquids: Effect of temperature and alkyl chain length on anion. *Fluid Phase Equilib.* **2015**, *386*, 65−74.
(25) Okoturo, O. O.; VanderNoot, T. J. Temperature dependence of viscosity for room temperature ionic liquids. *J. Electroanal. Chem.* **2004**, *568*, 167−181.
(26) Chhotaray, P. K.; Gardas, R. L. Structural Dependence of Protic Ionic Liquids on Surface, Optical, and Transport Properties. *J. Chem. Eng. Data* **2015**, *60*, 1868−1877.


DOI: 10.1021/acs.jced.5b00936
*J. Chem. Eng. Data* 2016, 61, 2260−2268